COMPUTED TOMOGRAPHIC IMAGING OF DOGS WITH PRIMARY LARYNGEAL OR TRACHEAL AIRWAY OBSTRUCTION

KRYSTINA STADLER, SUSAN HARTMAN, JODI MATHESON, ROBERT O'BRIEN

Seventeen dogs with clinical signs attributable to nonneoplastic obstruction of the larynx, trachea, or large bronchi underwent computed tomography (CT) imaging. In 16 of the 17 dogs, CT was performed without general anesthesia using a positioning device. Fifteen of these 16 dogs were imaged without sedation or general anesthesia. Three-dimensional (3D) internal rendering was performed on each image set based on lesion localization determined by routine image planes. Visual laryngeal examination, endoscopy, video fluoroscopy, and necropsy were used for achieving the cause of the upper airway obstruction. The CT and 3D internal rendering accurately indicated the presence and cause of upper airway obstruction in all dogs. CT findings indicative of laryngeal paralysis included failure to abduct the arytenoid cartilages, narrowed rima glottis, and air-filled laryngeal ventricles. Laryngeal collapse findings depended on the grade of collapse and included everted laryngeal saccules, collapse of the cuneiform processes and corniculate processes, and narrowed rima glottis. Trachea abnormalities included hypoplasia, stenosis, or collapse syndrome. The CT findings in tracheal hypoplasia consisted of a severely narrowed lumen throughout the entire length. Tracheal stenosis was represented by a circumferential decrease in tracheal lumen size limited to one region. Tracheal collapse syndrome was diagnosed by severe asymmetric narrowing. Lobar bronchi collapse appeared in CT images as a narrowed asymmetric lumen diameter. CT imaging of unanesthetized dogs with upper airway obstruction compares favorably with traditional definitive diagnostic methods. © 2011 *Veterinary Radiology & Ultrasound, Vol. 52, No. 4, 2011, pp 377–384.*

Key words: brachycephalic, bronchi, dyspnea, larynx, trachea.

Introduction

UPPER AIRWAY OBSTRUCTION is impedance of airflow at the level of the larynx, pharynx trachea, or primary bronchi.[1,2] For this study, the upper airway was defined as the airway proximal to and including the primary bronchi.

Radiographic evaluation of upper airway obstruction is limited because of superimposition and its static nature. A visual laryngeal examination or endoscopy may not be suitable because of the requirement for sedation or general anesthesia and possible need for corrective surgery or tracheostomy before recovery from anesthesia. Computed tomography (CT) has been used to evaluate dynamic airway changes in dogs under general anesthesia.[3] It would be beneficial to be able to use CT without the need for anesthesia.

Our purposes were twofold. To (1) describe the CT and three-dimensional (3D) internal rendered endoscopy findings in awake or sedated dogs with suspected upper airway obstruction and (2) evaluate the correlation between the CT imaging findings and the definitive diagnosis.

Materials and Methods

Dogs with respiratory distress attributable to upper airway obstruction examined between May 2009 and November 2010 were assessed. Seventeen dogs had one or more of the following clinical signs: dyspnea, increased upper airway sounds, cough, stridor, exercise intolerance, and gagging. Breeds represented were Pug (4), Yorkshire terrier (4), English bulldog (3), Chihuahua, Boston terrier, Brussels griffon, French bulldog, Pomeranian, and Rhodesian ridgeback. There were 10 females (nine neutered, one intact) and seven males (all neutered). The mean age was 6.7 years (range 3 months to 16 years) and the mean weight was 9.0 kg (range 1.5–32 kg).

The diagnosis was obtained using the following methods. Eleven dogs had a visual laryngeal examination using sedation or general anesthesia. Two dogs had evaluation of the trachea with video fluoroscopy. One dog had visual laryngeal exam, video fluoroscopy and endoscopy. Three dogs were euthanized and had a necropsy as the only diagnostic test.

Eleven of the 17 dogs were radiographed. All radiographed dogs had left and right lateral views and either dorsoventral or ventrodorsal views, nine dogs had a lateral view of the entire trachea added to the radiographic study

From the Department of Veterinary Clinical Medicine, University of Illinois at Urbana-Champaign, 1008 W. Hazelwood Dr, Urbana, Illinois 61802.

Presented in part at the EVDI Annual Meeting 2010.

Address correspondence and reprint requests to Robert O'Brien, at the above address. E-mail: bobrien@illinois.edu

Received December 6, 2010; accepted for publication February 18, 2011.

doi: 10.1111/j.1740-8261.2011.01816.x

and seven dogs had an expiratory lateral thoracic view added to the conventional three-view thoracic and tracheal study.

All patients underwent head, neck, and thoracic CT examination using a 16-slice helical CT scanner.* Sixteen of the 17 dogs were imaged in sternal recumbency in a transparent positioning device.† The device has ports on each end for catheter lines and supplemental oxygen allowing imaging without secation or anesthesia. The animals were monitored visually throughout the imaging procedure and all received supplemental oxygen during the CT examination. Two dogs were sedated to decrease anxiety and prevent excessive movement during imaging; one received dexmedatomidine‡ and both received butorphanol.§ In one dog, the CT images were not acquired using the positioning device due to the large body mass.

All dogs were scanned with a gantry rotation of 0.5 s. The kVp, mA, pitch, table speed, and field of view varied based on size and movement of the patient. For brachycephalic breeds approximately 1 ml of barium paste was placed on the base of the tongue by a wooden applicator to allow better distinction between the tongue and soft palate.

If severe motion artifact was observed, the CT examination was repeated. Image data were evaluated on a separate CT workstation to obtain symmetric transverse plane images. Subsequent multiplanar reformatting was performed to obtain dorsal and sagittal images, reconstructed with a 0.625 mm slice thickness, 0.312 mm slice reconstruction interval, and detail algorithm.

3D internal rendering was performed using appropriate CT software,¶ to create virtual endoscopic images of suspected lesions. To increase ease of creating the 3D internal rendering images and reduce artifact production, CT examinations were repeated in dogs with turned neck, severe motion artifact, or excessive barium in the oroesophageal region. Threshold of the 3D internal rendered images were adjusted based on the attenuation of the airway wall. Aperture of the images was adjusted after thresholding to allow for appropriate telescoping of the airway segment. The virtual endoscopy began rostral to the pharynx and continued through the principal and lobar bronchi, as clinically indicated.

The 3D internal rendering image of the larynx was obtained at the level of the basihyoid bone in the transverse plane (Fig. 1). To increase the likelihood of imaging the dynamic laryngeal lesion in the most severely affected phase of respiration, dogs were scanned multiple times. 3D internal rending images of the larynx were created for each image acquisition. The 3D internal rendering image that demonstrated the most severe phase of the dynamic lesion was presumed to be during inspiration for laryngeal collapse and paralysis.

The radiographs and CT images were evaluated independently by two board-certified radiologists (R.T.O., J.S.M.). Findings from one modality were not known when the images of the same patient from the other modality were evaluated. The CT imaging diagnosis was divided into the following four categories: laryngeal collapse, laryngeal paralysis, and tracheal stenosis or tracheal collapse syndrome. The CT findings and definitive diagnosis were compared for correlation.

Results

Radiographic findings in the 11 dogs imaged with this modality were hypoinflated lungs ($n = 7$), tracheal narrowing at the thoracic inlet ($n = 4$) and tracheal hypoplasia ($n = 1$). Of the seven dogs with additional expiratory-phase radiographs, no additional findings were seen.

The findings in the nine dogs with a lateral neck radiograph included increased soft tissue opacity in the larynx ($n = 4$), air-filled laryngeal ventricles ($n = 3$), thickened soft palate ($n = 1$), elongated soft palate ($n = 1$), and suspected intraluminal tracheal mass ($n = 1$). Four of the nine dogs had a diagnosis of laryngeal collapse. All these dogs had increased soft tissue opacity of the larynx and no visible air-filled lateral ventricles. Three of the nine dogs had a final diagnosis of laryngeal paralysis. All of these patients had air-filled, or subjectively air-dilated, laryngeal ventricles. Two of the nine dogs had a final diagnosis of tracheal collapse. One dog with tracheal collapse had an intraluminal or extramural mass suspected on radiographic and video fluoroscopic imaging. However, none of the three dogs with tracheal collapse had expiratory-phase radiographs.

CT protocols were altered according to patient size and the amount of patient movement during the scan and were recorded for 16 (of 17) patients. The kVP was 100 (9) or 120 (7) kVP and mA ranged from 120 to 350 (median = 235). The pitch was 0.93 ($n = 3$), 1.375 ($n = 6$), or 1.75 ($n = 7$) corresponding with a table speed of 9.3, 13, and 17 mm/s, respectively. The field of view was small ($n = 6$) or large ($n = 10$), depending on patient size. 3D internal rendering aperture varied per frame from 80 or 90 and threshold ranged from −200 to −600 HU. The patients were classified based on the site and type of the clinically most severe lesion identified with CT as laryngeal collapse, laryngeal paralysis, tracheal stenosis or tracheal collapse. Laryngeal collapse was present in nine dogs and all were brachycephalic. The most common breeds were the pug ($n = 3$) and English bulldog ($n = 3$) with one each Boston terrier, Brussels griffon, and French bulldog. Age ranged from 0.25 to 13 years with a mean of 5.3 years. Two

*GE Healthcare, Buckinghamshire, UK.
†VetMouseTrap™, University of Illinois, Urbana, IL.
‡Dexdormitor™, Pfizer, New York, NY, IM.
§Torbugesic™, Fort Dodge, IA, IM (1), IV (2).
¶Navigator Smooth, GE Healthcare.

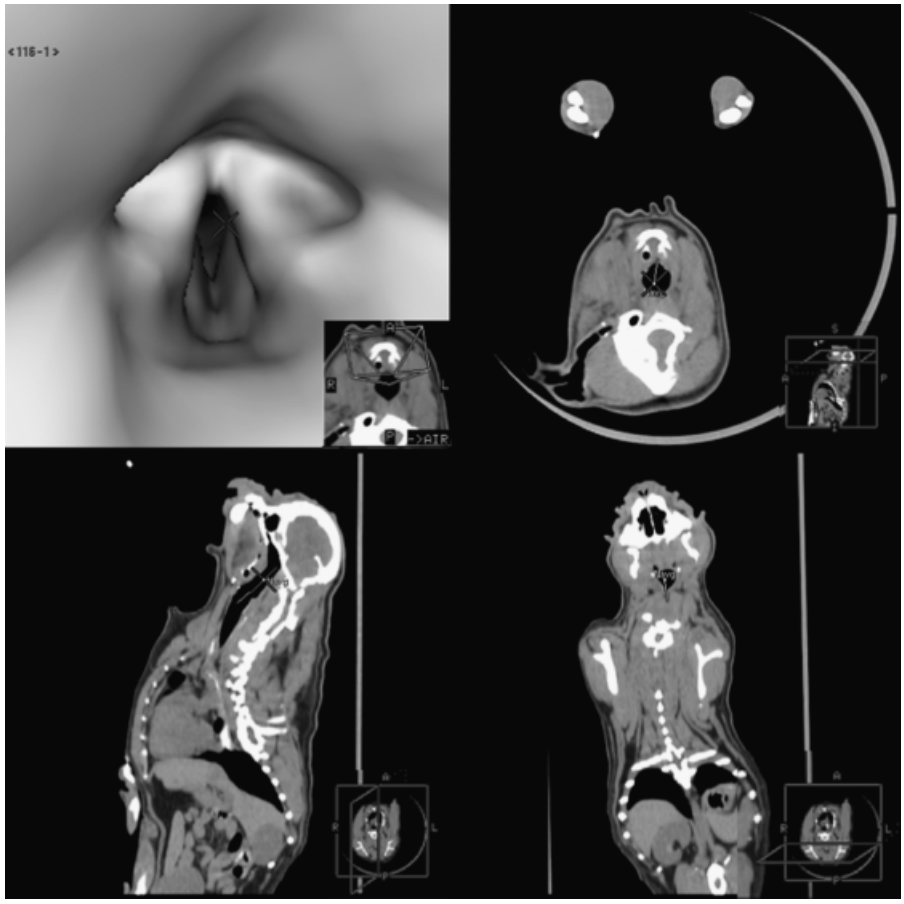

FIG. 1. Computed tomography (CT) work station screen images of three-dimensional volume rendering of the larynx. There is grade I laryngeal collapse at presumed expiration.

of these dogs were English bulldog puppies with concurrent severe tracheal hypoplasia. Both were euthanized and in addition to laryngeal collapse and tracheal hypoplasia there was noncardiogenic pulmonary edema on necropsy.

Laryngeal collapse was graded on CT images and visual laryngeal examination based on the Leonard grading system[4]: everted laryngeal saccules (grade 1), medial collapse of the cuneiform process of the arytenoid cartilages (grade 2), or medial collapse of the cuneiform and ventral collapse corniculate processes of the arytenoid cartilages (grade 3). Laryngeal collapse was assessed most accurately with the 3D internal volume rendered image of the larynx (Fig. 1). No routine MPR projection provided diagnostic information. Four dogs had grade 1 collapse, three had grade 2 collapse, and two had grade 3 collapse (Fig. 2). Dogs with laryngeal collapse had the following additional findings; lobar bronchial collapse ($n = 3$), elongated soft palate ($n = 3$), tracheal hypoplasia ($n = 2$), and tracheal collapse ($n = 1$). Diagnosis of laryngeal collapse was confirmed with a visual laryngeal examination ($n = 7$) or necropsy ($n = 2$). In two dogs, the grade of collapse differed between CT and laryngeal examination. One dog with grade II laryngeal collapse on CT had grade III collapse on visual laryngeal exam. Another dog diagnosed with grade II collapse from CT, had grade I collapse on necropsy. In one dog with grade 3 laryngeal collapse based on CT findings, there was no mention of laryngeal disease in the necropsy report.

Four dogs had laryngeal paralysis. There were two Yorkshire terriers, one Chihuahua, and one Rhodesian ridgeback. Laryngeal paralysis was detected most accurately using the 3D volume rendered view of the larynx. CT findings of all patients with laryngeal paralysis included failure to abduct the arytenoid cartilages and collapse into the rima glottis on presumed inspiration, stenosis of the laryngeal inlet and air-filled lateral ventricles (Fig. 3). In the 3D internal rendering program, the dilated lateral ventricles were processed as being contiguous with and lateral to the adducted vocal folds. This problem, while providing inaccurate anatomic information, augmented the ability to evaluate arytenoid adduction and lateral ventricle air dilation concurrently on a single CT image. All dogs with laryngeal paralysis had diagnostic confirmation with a visual laryngeal examination.

Six dogs had tracheal abnormalities, including tracheal collapse syndrome ($n = 3$), tracheal hypoplasia ($n = 2$), and focal stenosis ($n = 1$). Both dogs with tracheal hypoplasia

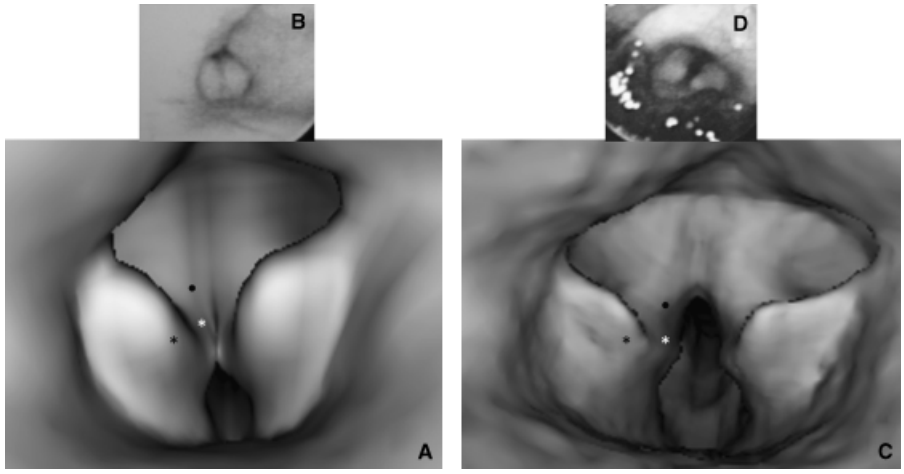

FIG. 2. (A) Three-dimensional volume rendering of the larynx at the level of the laryngeal inlet at presumed inspiration. Grade 3 laryngeal collapse was diagnosed based on everted laryngeal saccules (white asterisk), collapse of the cuneiform (black asterisk), and corniculate processes (black dot). (B) Laryngoscopy image of the dog in (A) where grade 3 laryngeal collapse at presumed inspiration is confirmed. (C) Three-dimensional volume rendering of larynx and (D) laryngoscopy image of the same dog during presumed expiration. Note less severe cuneiform (black asterisk) and corniculate (black dot) process collapse, but persistent everted laryngeal saccules (white asterisk).

were juvenile English bulldogs with severe brachycephalic syndrome, including laryngeal collapse. Both dogs had tracheal hypoplasia confirmed by necropsy. All dogs with tracheal collapse had the diagnosis confirmed using video fluoroscopy. One dog had additional grade I laryngeal collapse and one dog had left cranial and caudal lobar bronchi collapse. Breeds with tracheal collapse included Pomeranian, Pug, and Yorkshire terrier.

MPR and 3D internal rendering projections were complimentary for imaging tracheal lesions. Clinicians related better to the 3D internal rendering images they appeared similar to endoscopic images. Routine transverse images were adequate for the diagnosis of a tracheal lesion in all dogs and for differentiation between collapse, stenosis, and hypoplasia. Additional sagittal and dorsal plane projections provided better information on the length of the affected segment. Tracheal hypoplasia appeared as static generalized symmetric (round in cross-section) narrowing of the tracheal lumen throughout its entire length. Focal stenosis of the tracheal diameter in one dog was characterized by a focal symmetric (radial) decrease in tracheal lumen size. Tracheal collapse syndrome was diagnosed by asymmetric narrowing (curved ellipse) of the trachea (Fig. 4). All tracheal collapse occurred at the thoracic inlet.

Lobar bronchial collapse was present in four dogs. Collapse was defined as a height to width ratio of >2 of the lobar bronchi (Fig. 5). Dogs with lobar bronchial collapse also had either laryngeal collapse ($n=3$) or tracheal collapse ($n=1$). All four dogs had collapse in the bronchus of the cranial segment of the left cranial lobe. Other affected

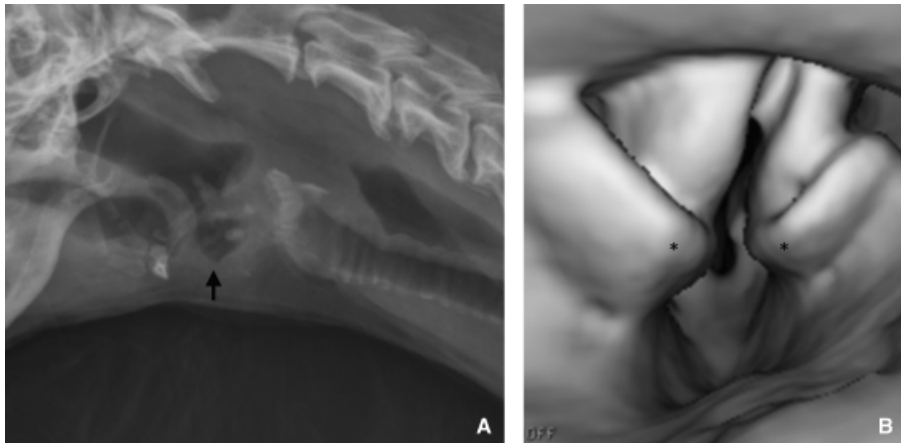

FIG. 3. Lateral radiograph (A) of a dog with laryngeal paralysis. Note the air-filled laryngeal ventricles (black arrow). Three-dimensional internal volume rendering of larynx (B). Note the collapse of the arytenoid cartilages (asterisks) into the rima glottis due to with laryngeal paralysis.

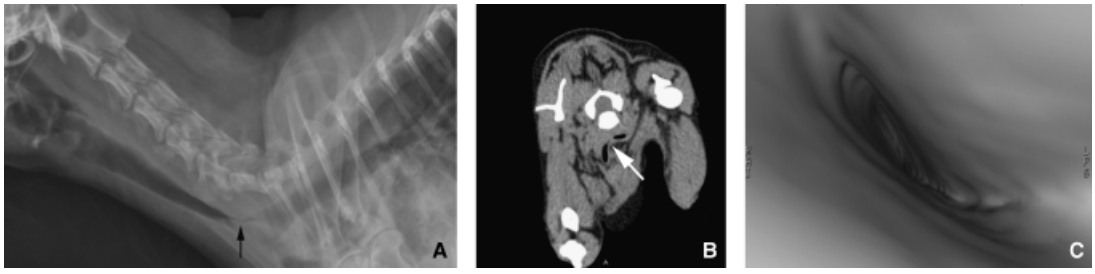

FIG. 4. (A) Left lateral radiograph. Note the severe narrowing of the trachea at the thoracic inlet with suspect round soft tissue mass lesion (black arrow). Transverse computed tomography (CT) (B) and virtual endoscopy (C) images at the thoracic inlet. Note the asymmetric collapse of the trachea (white arrow) and no mass lesion.

bronchi were the bronchus of the caudal segment of the left cranial lung lobe ($n = 3$), left caudal lobar bronchus ($n = 3$), and right middle lobar bronchus ($n = 1$). No dog with laryngeal paralysis had lobar bronchial collapse.

Elongated soft palate appeared on sagittal CT images as the soft palate extending caudal to the cranial tip of the epiglottis. Three dogs had elongated soft palate and all were brachycephalic breeds and also had laryngeal collapse.

Discussion

CT is an important diagnostic tool for evaluating upper airway obstruction in human patients.[5–8] 3D internal rendering of CT images into virtual endoscopy are used to improve the interpretation of the airway's intraluminal anatomy. There are certain disadvantages when displaying the airways as a series of transverse images. These are the large number of images, poor representation of oblique structures lying in nonorthogonal planes, difficult evaluation of the tissue interfaces and surfaces parallel to the transverse plane, and poor representation of pathologic processes and anatomic structures lying in multiple planes. Virtual endoscopy can effectively support the transverse images and aid in the diagnosis of upper airway disease.[7,9] Results of these imaging studies closely mirror traditional endoscopic findings.[10,11]

The value of CT in dogs with upper airway obstruction has been limited by the presence of the endotracheal tube (ET) used to support general anesthesia. The ET interferes with luminal measurements, both on transverse images and 3D internal rendering, by mechanical effects and also because of the dynamic effect of positive pressure ventilation.

In this study, 17 dogs had CT performed without ET placement. The CT and 3D internal rendering images allowed for assessment of the upper airway for signs of laryngeal collapse and paralysis, tracheal collapse, hypoplasia and stricture and principal and lobar bronchi collapse. 3D volume renderings allowed assessment of the cranial aspect of the larynx. 3D internal rendering was challenging to construct, produced artifacts and led to rescanning in dogs to correct one or more of the following issues: turned neck, motion, or excessive barium in the oropharyngeal region. Neck twist and head motion affect the luminal placement between each slice during internal rendering image acquisition and distort the accuracy with which the volume rendering software locates the lumen. In 3D internal rendering, a specific attenuation coefficient is chosen as a threshold to define the air–lumen interface, therefore all voxels are air or soft tissue, without an identifiable transition zone.[12] Conditions such as pharyngeal barium, decreased lumen diameter, and air-filled laryngeal ventricles altered the air–lumen interface and, therefore, affected image quality. Also, the phase of respiration at which a particular transverse image was acquired was unknown. Dogs with dynamic lesions were scanned multiple times to increase the likelihood of imaging during

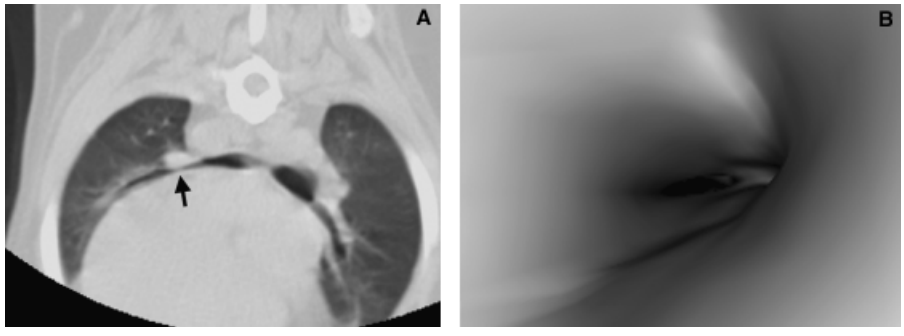

FIG. 5. Transverse computed tomography (CT) image (A). Note the collapse of the primary bronchus of the cranial subsegment of the left cranial lung lobe (black arrow). Virtual bronchoscopy image (B) at same location. Note the severe asymmetric narrowing of the bronchial lumen.

the phase of respiration when the lesion was most severe. The image set in which the most severe lesion was noted was the one used for reconstruction, using both the MPR and 3D internal rendering techniques. Since the lesion was most severe during this scan, the lesions were presumed to be either static or imaged during inspiratory phase of respiration.

All dogs with laryngeal collapse had increased laryngeal soft tissue opacity on lateral neck radiographs. This finding has not been previously reported. CT diagnosis required 3D internal rendering to image the laryngeal components clearly and, therefore, grade the collapse (Fig. 1). All dogs with laryngeal collapse were diagnosed correctly based on 3D internal rendering CT. The MPR projections in dogs with laryngeal paralysis and laryngeal collapse provided no diagnostic information. Without 3D internal rendering, the reviewers were unable to assess laryngeal paralysis or collapse accurately.

All dogs with laryngeal collapse were brachycephalic. Laryngeal collapse is a component of brachycephalic airway syndrome.[4,13,14] CT findings of elongated soft palate, tracheal collapse, and lobar bronchi collapse in patients with laryngeal collapse are additional findings associated with brachycephalic airway syndrome.[4,13–15] Two English bulldogs with laryngeal collapse had concurrent tracheal hypoplasia seen on CT images and found at necropsy. English bulldogs are predisposed to tracheal hypoplasia.[16]

All dogs diagnosed with laryngeal paralysis that underwent lateral cervical radiography had air-dilated laryngeal ventricles. CT image findings included stenosis of the laryngeal inlet and air-filled lateral ventricles. 3D internal rendering was necessary to assess the arytenoid cartilages. The 3D laryngeal images of dogs with laryngeal paralysis were presumed to be inspiratory based on failure of arytenoid cartilage abduction and collapse into the rima glottis, a lesion seen only during inspiration.[17] To increase chances of an inspiratory laryngeal scan, multiple scans were performed on these patients. Laryngeal paralysis could be diagnosed falsely as a normal larynx if images were not acquired during the correct respiratory phase. During visual or endoscopic laryngeal examinations, the respiratory phase is known and laryngeal paralysis is diagnosed during inspiration.[18,19] All patients diagnosed with laryngeal paralysis on CT were diagnosed with laryngeal paralysis using visual or endoscopic laryngeal examination, correlating with the presumption that the 3D laryngeal image was taken during inspiration.

Laryngeal paralysis is either inherited or acquired. The hereditary form is reported commonly in Bouvier des Flanders,[20] less commonly in the Bull terrier, Malamute, and Siberian Husky breeds.[17] The acquired, idiopathic form is most commonly a disease of older medium to giant breed dogs although it has been described in small breeds of dogs.[18,21] All instances of laryngeal paralysis in this study were thought to be acquired. Three of the four dogs with laryngeal paralysis were small breed dogs. Yorkshire terrier ($n = 2$) has been previously described as being at risk laryngeal paralysis.[21] Laryngeal paralysis has not been described in Chihuahua dogs. Small breed dogs may have been overrepresented in this study due to size limitations of the positioning device. Two of the dogs with laryngeal paralysis were sedated for CT imaging. Sedation was both for therapy and to limit motion. Too deep a level of sedation has potential to restrict arytenoid movement, affecting accurate diagnosis.[18,19] All sedated dogs were diagnosed with laryngeal paralysis visually in a separate laryngeal examination, using similar sedation.

Tracheal collapse, hypoplasia, and stenosis diagnosed by CT were comparable to the diagnosis made by alternative diagnostic methods. In a Pug with tracheal collapse, grade I laryngeal collapse was also diagnosed using CT. Additionally, left cranial and caudal lobar bronchial collapse was seen on CT imaging but not seen on video fluoroscopy. Lobar bronchi collapse, a finding consistent with tracheal collapse syndrome, was seen on CT in one dog with tracheal collapse.[22,23]

Lobar bronchi collapse was present in three (of nine) dogs of laryngeal collapse and one (of three) dog with tracheal collapse. All instances of lobar bronchi collapse included collapse of the cranial lobar bronchus of the left cranial lung lobe. Left cranial lobar bronchus is the most common bronchus affected in brachycephalic airway syndrome.[13,15]

The imaging protocol for dogs with suspected laryngeal collapse and paralysis and normal thoracic radiographs should began with a lateral cervical radiograph (Fig. 6). Laryngeal collapse is radiographically characterized by an increase in soft tissue opacity in the region of the lateral ventricle. This contrasts with dogs with laryngeal paralysis in which the lateral ventricles of the larynx are air-filled. These radiographic findings have not been previously reported and may be clinically useful for the radiographic evaluation of laryngeal disease. However, these findings are not specific and CT 3D internal volume provides additional information (Fig. 6).

A major limitation was the inability to obtain CT images during a given phase of respiration. All lesions were presumed to be static or imaged in inspiration based on lesion appearance in repeated CT scans. Mild disease or dynamic lesions could go undetected if imaged in the wrong phase of respiration. This may account for differences in laryngeal collapse grading in CT compared with more definitive methods. Respiratory gating would allow for dogs to be images at a given phase of respiration.[24–26] Capturing a given respiratory phase in the larynx would require a dynamic CT study of a large region of the larynx. Maintaining high resolution using a 16-slice CT scanner limits the region being scanned to 1.0 cm (16 slices $\times$ 0.625 mm slice thickness). Gating is not currently available for our imaging system.

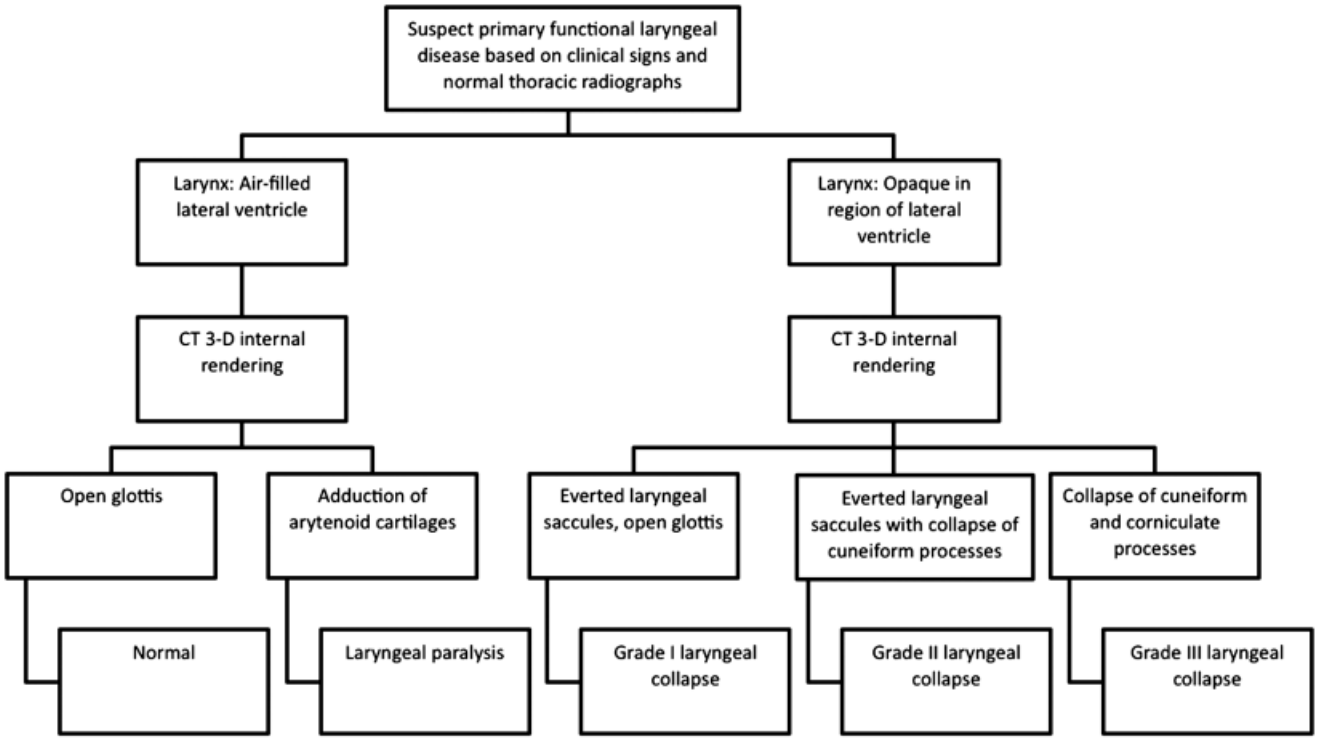

FIG. 6. Flow chart of decision protocol for imaging dogs with suspected laryngeal obstruction.

In conclusion, CT imaging of nonanesthetized dogs with upper airway obstruction in a restraining device without chemical restraint is a noninvasive method of achieving a definitive diagnosis of upper airway obstruction.

REFERENCES

1. Stedman TL. The American heritage Stedman's medical dictionary. Harcourt: Houghton Mifflin, 2004.

2. Lee JA, Drobatz KJ. Respiratory Distress and Cyanosis in Dogs. (Chapter 1). In: King LG (ed): Textbook of respiratory disease in dogs and cats. Philadelphia: WB Saunders Co, 2004;4.

3. Leonard CD, Johnson LR, Bonadio CM, et al. Changes in tracheal dimensions during inspiration and expiration in healthy dogs as detected via computed tomography. Am J Vet Res 2009;70:986–991.

4. Leonard HC. Collapse of the larynx and adjacent structures in the dog. J Am Vet Med Assoc 1960;137:360–363.

5. Polo O, Tafti M, Fraga J, et al. Pharyngeal CT studies in patients with mild or severe upper airway obstruction during sleep. Sleep 1993;16(Suppl): S152–S155.

6. Salvolini L, Bichi Secchi E, Costarelli L, et al. Clinical applications of 2D and 3D CT imaging of the airways: a review: from diagnosis to therapy. Eur J Radiol 2000;34:9–25.

7. Silverman P, Zeiberg A, Troost T, et al. Three-dimensional imaging of the hypopharynx and larynx by means of helical (spiral) computed tomography: comparison of radiological and otolaryngological evaluation. Ann Otol Rhinol Laryngol 1995;104:425–431.

8. Brasch R, Gould R, Gooding C, et al. Upper airway obstruction in infants and children: evaluation with ultrafast CT. Radiology 1987;165: 459–466.

9. Silverman PM, Zeiberg AS, Sessions RB, et al. Helical CT of the upper airway: normal and abnormal findings on three-dimensional reconstructed images. Am J Roentgenol 1995;165:541–546.

10. Salvolini L, Gasparini S, Baldelli S, et al. Virtual bronchoscopy: the correlation between endoscopic simulation and bronchoscopic findings. Radiol Med 1997;94:454–462.

11. Lee KS, Yoon JH, Kim TK, et al. Evaluation of tracheobronchial disease with helical CT with multiplanar and three-dimensional reconstruction: correlation with bronchoscopy. RadioGraphics 1997;17:555–567.

12. Naidich DP, Webb WR, Grenier PA. Imaging of the airways: functional and radiologic correlations. Philadelphia, PA: Lippincott, Williams & Wilkins, 2005.

13. De Lorenzi D, Bertoncello D, Drigo M. Bronchial abnormalities found in a consecutive series of 40 brachycephalic dogs. J Am Vet Med Assoc 2009;235:835–840.

14. Wykes PM. Brachycephalic airway obstructive syndrome. Probl Vet Med 1991;3:188–197.

15. Bernaerts F, Talavera J, Leemans J, et al. Description of original endoscopic findings and respiratory functional assessment using barometric whole-body plethysmography in dogs suffering from brachycephalic airway obstruction syndrome. Vet J 2010;183:95–102.

16. Coyne BE, Fingland RB. Hypoplasia of the trachea in dogs: 103 cases (1974–1990). J Am Vet Med Assoc 1992;201:768–772.

17. Aron DN, Crowe DT. Upper airway obstruction. Vet Clin N Am Small Anim Pract 1985;15:891–917.

18. Holt D, Brockman D. Diagnosis and management of laryngeal disease in the dog and cat. Vet Clin N Am Small Anim Pract 1994;24: 855–871.

19. Smith MM. Diagnosing laryngeal paralysis. J Am Anim Hosp Assoc 2000;36:383–384.

20. Venker-van Haagen AJ, Hartman W, Goedegebuure SA. Spontaneous laryngeal paralysis in young Bouviers. J Am Vet Med Assoc 1978;172:714–716.

21. Gaber CE, Amis TC, LeCouteur RA. Laryngeal paralysis in dogs: a review of 23 cases. J Am Vet Med Assoc 1985;186:377–380.

22. Johnson L. Tracheal collapse. Diagnosis and medical and surgical treatment. Vet Clin N Am Small Anim Pract 2000;30:1253–1266.

23. Hedlund CS. Tracheal collapse. Probl Vet Med 1991;3:229–238.

24. Ford E, Mageras G, Yorke E, et al. Respiration-correlated spiral CT: a method of measuring respiratory-induced anatomic motion for radiation treatment planning. Med Phys 2003;30:88–97.

25. Ford E, Mageras G, Yorke E, et al. Evaluation of respiratory movement during gated radiotherapy using film and electronic portal imaging. Int J Radiat Oncol Biol Phys 2002;52:522–531.

26. Ritchie CJ, Hsieh J, Gard MF, et al. Predictive respiratory gating: a new method to reduce motion artifacts on CT scans. Radiology 1994; 190:847–852.